Rough eye Is a Gain-of-Function Allele of *amos* That Disrupts Regulation of the Proneural Gene *atonal* During Drosophila Retinal Differentiation

Françoise Chanut,*[,1,2] Katherine Woo,*[,1] Shalini Pereira,[†,3] Terrence J. Donohoe,[†,4] Shang-Yu Chang,[‡,5] Todd R. Laverty,[§] Andrew P. Jarman and Ulrike Heberlein*[,††]**

**Department of Anatomy, [†]Gallo Center and [††]Program in Neuroscience and Developmental Biology, University of California, San Francisco, California 94143, [‡]Cornell Graduate School of Medical Sciences, Sloan-Kettering Research Institute, New York, New York 10021, [§]Department of Molecular and Cell Biology, Howard Hughes Medical Institute, University of California, Berkeley, California 94720 and **Wellcome Trust Center for Cell Biology, Institute of Cell and Molecular Biology, University of Edinburgh, Edinburgh EH9 3JR, United Kingdom*

Manuscript received September 7, 2001
Accepted for publication November 21, 2001

ABSTRACT

The regular organization of the ommatidial lattice in the Drosophila eye originates in the precise regulation of the proneural gene *atonal* (*ato*), which is responsible for the specification of the ommatidial founder cells R8. Here we show that *Rough eye* (*Roi*), a dominant mutation manifested by severe roughening of the adult eye surface, causes defects in ommatidial assembly and ommatidial spacing. The ommatidial spacing defect can be ascribed to the irregular distribution of R8 cells caused by a disruption of the patterning of *ato* expression. Disruptions in the recruitment of other photoreceptors and excess Hedgehog production in differentiating cells may further contribute to the defects in ommatidial assembly. Our molecular characterization of the *Roi* locus demonstrates that it is a gain-of-function mutation of the *bHLH* gene *amos* that results from a chromosomal inversion. We show that *Roi* can rescue the retinal developmental defect of ato^1 mutants and speculate that *amos* substitutes for some of *ato*'s function in the eye or activates a residual function of the ato^1 allele.

THE compound eye of *Drosophila melanogaster* is a regular array of ~800 ommatidia, each composed of 8 photoreceptor cells (R1–R8) and 12 accessory cells (Wolff and Ready 1993). The development of each ommatidium begins with the specification of an R8 photoreceptor precursor (Tomlinson and Ready 1987a,b). The R8 precursor acts as a founder cell around which all other ommatidial cell types are progressively recruited through a series of inductions mediated by Sevenless (Sev) and the epidermal growth factor receptor (EGFR; Tomlinson *et al.* 1987; Freeman 1997). Retinal differentiation begins at the posterior margin of the eye-antennal disc in early third instar larvae and proceeds as a wave that reaches the anterior disc margin by the early pupal stage, ~48 hr later (Wolff and Ready 1993). At the front of the differentiation wave, an indentation in the epithelium known as the morphogenetic furrow (MF) marks the transition between proliferating, undifferentiated cells in the anterior and differentiating cells in the posterior. In the MF, cells are arrested at the G1 phase of the cell cycle (Ready *et al.* 1976; Tomlinson 1985; Wolff and Ready 1993). Retinal neurogenesis begins with the broad expression of the proneural gene *atonal* (*ato*; Jarman *et al.* 1993) in all cells of the furrow's anterior edge, followed by the progressive restriction of *ato* in the MF, eventually leading to the resolution of single *ato*-expressing R8 precursors at the furrow's posterior edge (Jarman *et al.* 1994; Dokuçu *et al.* 1996; Sun *et al.* 1998). *ato* encodes a basic-helix-loop-helix (bHLH) protein with high sequence similarity to proneural proteins of the Achaete-Scute family (Jarman *et al.* 1993). Like other members of this group, Ato is thought to exert its proneural function via its dimerization with the bHLH protein Daughterless (Da; Jarman *et al.* 1993; Brown *et al.* 1996). In spite of its broad expression pattern, *ato* is only strictly required for the specification of the R8 precursors (Jarman *et al.* 1994) and for some aspects of their differentiation into R8 photoreceptors (White and Jarman 2000). Nevertheless, in the absence of *ato* function, all retinal cell types are missing because of the absence of ommatidial founders (Jarman *et al.* 1994). Whether additional proneural genes specify the other photoreceptor fates is currently unknown.

Expression of *ato* is tightly controlled temporally and spatially, which reflects complex patterning mechanisms that ultimately ensure the regular spacing of nascent ommatidia behind the MF (Heberlein and Moses 1995; Brennan and Moses 2000). *ato* is activated in the MF by the diffusing factor Hedgehog (Hh; Domínguez and Hafen 1997; Strutt and Mlodzik 1997; Borod and

[1]These authors contributed equally to this work.

[2]*Corresponding author:* Department of Anatomy, S1334, Box 0452, University of California, 513 Parnassus Ave., San Francisco, CA 94143. E-mail: chanut@itsa.ucsf.edu

[3]*Present address:* Department of Laboratory Medicine, University of California, San Francisco, CA 94143.

[4]*Present address:* Boston University School of Medicine, Boston, MA 02118.

[5]*Present address:* ITRI-BMEC, Hsinchu 310,Taiwan.

Heberlein 1998; Domínguez 1999), which is synthesized by photoreceptors differentiating behind the MF (Heberlein *et al.* 1993; Ma *et al.* 1993) and repressed anterior to the MF by the neuronal inhibitors *hairy* (*h*) and *extramacrochaete* (*emc*; Brown *et al.* 1995). The transmembrane receptor Notch (N; Wharton *et al.* 1985) and its ligands Delta (Dl; Kopczynski *et al.* 1988) and Scabrous (Sca; Lee *et al.* 1996; Powell *et al.* 2001) then pattern *ato*'s profile via a process of lateral inhibition: *ato* expression is first restricted to evenly spaced intermediate groups at the posterior edge of the MF and eventually to single R8 precursors that emerge at regular intervals behind the MF (Baker and Zitron 1995; Baker *et al.* 1996; Sun *et al.* 1998; reviewed in Brennan and Moses 2000). Resolution and spacing of single R8 precursors are in addition controlled by the homeodomain protein Rough (Ro; Tomlinson *et al.* 1988; Heberlein *et al.* 1991) that keeps *ato* transcription repressed in cells other than R8 (Dokuçu *et al.* 1996). *ato* also regulates its own expression and is required to maintain high levels of Ato protein in the intermediate groups and R8 precursors (Sun *et al.* 1998).

A number of mutations are known to disrupt the regular arrangement of the eye facets, causing roughening of the eye surface. While many affect the recruitment or specification of the various ommatidial cell types induced by the R8 founders (reviewed in Albagli *et al.* 1997; Kumar and Moses 1997), several have been traced back to early patterning defects in the MF (Baker *et al.* 1990; Baker and Rubin 1992; Cagan 1993; Thomas *et al.* 1994). *Rough eye* (*Roi*) has been known for many years as a dominant mutation that causes roughening of the eye surface (Renfranz and Benzer 1989; Heberlein *et al.* 1993). On the basis of their observation of adult retinal sections and MF cell morphology, Renfranz and Benzer (1989) proposed that *Roi* disrupted early patterning in the MF. Consistent with this proposal, we previously reported that *Roi* acts as a strong suppressor of two mutations that cause a premature arrest of furrow progression, hh^{bar3} and ro^{Dom} (Heberlein *et al.* 1993). We showed that *Roi* restored the anterior progress of retinal differentiation and the expression of a furrow-specific reporter gene in both mutant backgrounds. hh^{bar3} is a hypomorphic allele with a regulatory region mutation that abolishes *hh* expression in the eye (Lee *et al.* 1992; Huang and Kunes 1996), leading to insufficient *ato* expression in the MF (F. Chanut and U. Heberlein, unpublished observation) and eventually to the arrest of the furrow (Chanut and Heberlein 1997). ro^{Dom} is a gain-of-function mutation that causes an anterior expansion of the domain of *ro* expression, leading to furrow arrest via the progressive repression of *ato* expression in the MF (Chanut *et al.* 2000). To understand how *Roi* might restore furrow progression in both of these backgrounds, we decided to characterize the molecular nature of the *Roi* mutation.

Here we describe our phenotypic and molecular characterization of the *Roi* mutation. We find that *Roi* disrupts *ato* patterning and increases *hh* expression behind the MF. We show that *Roi* is linked to a genomic inversion between cytological positions 36A and 37A that causes misexpression of the proneural gene *amos* in the eye. We show that experimental overexpression of *amos* in eye discs mimics the *Roi* phenotype and that *Roi* rescues retinal differentiation in homozygous *ato* mutants. We discuss various mechanisms for the effects of *Roi* and *amos* on *ato* expression and retinal patterning.

MATERIALS AND METHODS

Fly stocks and culture: *Roi* arose spontaneously in *In(2L)t* (22D3–E1; 34A8–9) but has also been introduced on the *CyO* balancer (Lindsley and Zimm 1992). For most genetic interactions and mapping purposes, we used a *Roi, CyO* chromosome obtained from the Bloomington Stock Center. For the analysis of the *Roi* phenotype in somatic clones, we used a chromosome where *Roi* had been separated from other rearrangements by homologous recombination (K. Harshman and D. Ballinger, unpublished data). Briefly, a recombinant chromosome (*al, b, Roi, pr, cn*) was recovered in 1 out of 15,000 progeny from females of the genotype $In(2L)Cy^{L}, t^{R}$, *Cy, Roi, pr/al, b, pr, cn*. This chromosome had no large chromosomal aberration and was used to isolate a second recombinant (*isoRoi*), in which the portions of the second chromosome located outside the *b-pr* interval were replaced by an isogenic, homozygous viable chromosome. Recombination mapping placed *Roi* at position 2-52.5, between *b* (2-48.5; cytological position 34D1) and *pr* (2-54.5; cytological position 38B4).

The ato^{1} mutation and *UAS-amos* construct have been described previously (Jarman *et al.* 1993; Goulding *et al.* 2000). da^{UX136} (synonym, da^{10}; Brown *et al.* 1996) was obtained from N. Brown; *hh-lacZ* (line P30; Lee *et al.* 1992), from P. Beachy; *dpp-lacZ* (line H1-1; Blackman *et al.* 1991), from R. Blackman; *hsFLP1* and *FRT(40)P[w^{+}]30C* (Xu and Rubin 1993), from G. Rubin; the *h-Gal4* line (*P{GAL4}*h^{H10}; Huang and Fischer-Vize 1996), from M. Mlodzik; the *dpp-Gal4* line (*P{GAL4-dpp.blk1}40C.6*; Staehling-Hampton *et al.* 1994), from J. Treisman; the *dac-Gal4* line (*P{GawB}*dac^{P7d23}; Heanue *et al.* 1999), from G. Mardon; the *GMR-Gal4* line (*P{GMR-GAL4.12}*; Freeman 1996), from M. Freeman; and hh^{13c} (synonym, hh^{81}; Jürgens *et al.* 1984), dpp^{blk} (synonym, $dpp^{d\text{-}blk}$; Blackman *et al.* 1987), the *hs-GAL4* line (*P{GAL4-Hsp70.PB}89-2-1*; Brand *et al.* 1994), *Df(2L)r10* (Ashburner *et al.* 1990; Schupbach and Wieschaus 1991), $Df(2L)cact^{255rv64}$ (Tower *et al.* 1993), *Df(2L)TW137*, and *Df(2L)TW50* (Wright *et al.* 1976), from the Bloomington Stock Center. All crosses were carried out at standard temperatures on standard fly medium.

Induction of somatic clones: Chromosomes where *Roi* was linked to *FRT(40)* [genotype *Roi, P[w^{+}], FRT(40)* or *Roi, FRT(40)*] were recovered in the progeny of *isoRoi/FRT(40)P[w^{+}]30C* females, after selection on neomycin (Xu and Rubin 1993). To generate homozygous *Roi* mutant clones in an *Roi* heterozygous background (Figure 1C), the following cross was performed: *hsFLP1; FRT(40), P[w^{+}]30C* × *FRT(40), Roi/CyO*. To generate wild-type clones in a *Roi* mutant background (Figure 1D), *Roi* was recombined onto the *FRT(40), P[w^{+}]30C* chromosome and the following cross performed: *hsFLP1; FRT(40), Roi, P[w^{+}]30C/CyO* × *FRT(40)*. Progeny were grown at 25° and subjected to a 1-hr heat shock at 38.5° once at the end of the first larval instar (48 hr after egg laying) and once at the end of the second larval instar (72 hr after egg laying). The presence of

homozygous *Roi* or wild-type clones was inferred from unpigmented patches in the background of w^+, *Roi* heterozygous eyes.

Mapping *Roi* against deficiencies: Although *Roi* had been reported to be lethal over deficiencies that spanned the 36–37 region (Lindsley and Zimm 1992), we were able to obtain viable *trans*-heterozygous escapers. The eye phenotype of the *trans*-heterozygotes proved difficult to interpret. For instance, *Df(2L)r10* (35D1; 36A6–7) caused a slight suppression of the rough eye phenotype, suggesting that it might uncover the gene responsible for *Roi*, assuming that *Roi* was a hypermorphic allele. However, an overlapping deficiency, *Df(2L)cact*^{255rv64} (35F6–12; 36D) had the opposite effect of slightly enhancing the rough eye phenotype, suggesting that it too might uncover the *Roi* gene, assuming that *Roi* was an antimorphic allele. Two more distal deficiencies, *Df(2L)TW137* (36C2–4; 37B9–10) and *Df(2L)TW50* (36E4–F1; 38A6–7) were also found to enhance the rough eye phenotype, while other deficiencies in the area had no detectable effect on *Roi*.

Interactions with *amos* also proved confusing: A recently generated loss-of-function allele (P. zur Lage and A. P. Jarman, unpublished results) causes a slight suppression of the rough eye phenotype, which is surprising since the wild-type *amos* gene is not expressed to detectable levels in the eye (Goulding *et al.* 2000). In addition, if an *amos* loss-of-function allele acts as a suppressor of *Roi*, one would have expected *Df(2L)TW137* and *Df(2L)TW50*, which remove the *amos* locus, to also act as suppressors, instead of enhancers. A simple interpretation of these contradictory observations is that the deficiency stocks, and perhaps the *amos* mutant stock as well, carry multiple lesions that can act as second-site modifiers of *Roi*. Consistent with this interpretation, we have found that *Roi* displays dominant interactions with many known and unknown loci (T. J. Donohoe, S. Pereira and U. Heberlein, unpublished observations).

Reversion of the *Roi* phenotype: Since the deficiency mapping did not allow us to understand either the nature of the *Roi* allele or its precise location, we attempted to map *Roi* by generating revertants. We first mutagenized *CyO, Roi/l(2)* flies with X rays and recovered four *CyO*-linked potential revertants out of 30,000 flies screened. Chromosome squashes of the phenotypic revertants showed cytological abnormalities in the 36–37 region, confirming the original mapping and showing that *Roi* could be reverted. To obtain molecular access to the *Roi* gene, we reverted *Roi* by hybrid dysgenesis (Engels 1989). *CyO, Roi/l(2)* virgin females were crossed to males of the π2 *P*-element donor stock. Their dysgenic male progeny (F_1) were then crossed to ry^{506} virgin females *en masse*, and the *CyO* progeny (F_2) were examined for eye roughness. Five *CyO*-linked mutations that eliminated (or strongly reduced) the roughness of *Roi* eyes were recovered out of ~100,000 F_2 screened. *In situ* hybridization to salivary gland chromosomes with *P*-element probes revealed that one of the five putative revertants carried a *P* element near 37 on the *CyO* chromosome, suggesting a revertant, rather than a second site suppressor of *Roi*. This mutant, referred to as Roi^{Rev}, also contained seven additional *P* elements. We were able to revert Roi^{Rev} to a rough-eye (presumably *Roi*) phenotype by remobilizing the *P* elements with the Δ2–3 transposase (Robertson *et al.* 1988), confirming that the reversion was due to a *P* insertion. Molecular analysis of 16 germ-line revertants of Roi^{Rev} established that all had lost the *P*-element insertion at 37. This confirmed that the gene responsible for the rough-eye phenotype mapped to the 37 region.

Molecular analysis of the 36A–37A region: Genomic DNA from Roi^{Rev} mutant flies was subjected to a partial *Sau*3A digest and cloned into a λ FIX *Bam*HI vector (Stratagene, La Jolla, CA). Phages that hybridized to *P*-element probes were isolated and hybridized in pools of 10 to wild-type salivary gland polytene chromosomes. Phages from pools that hybridized to the 36–37 region were retested individually. Several of them yielded two signals, one at 36A and one at 37A. This suggested that the *P* element in Roi^{Rev} had inserted near a chromosomal inversion between 36A and 37A. Phage DNAs that spanned the inversion breakpoint were used to isolate wild-type cosmid clones from a library kindly provided by John Tamkun. Several cosmids yielded two signals when hybridized to *Roi* chromosomes, though they hybridized to either 36A or 37A in wild type, confirming the presence of a chromosomal inversion in *Roi*. DNA sequencing of one of the phage clones from Roi^{Rev}, λ89, showed that the *P* element was inserted in DNA normally located at 36A, but translocated near 37A in *Roi*. Comparison with wild-type genomic sequences and the Drosophila genome sequence (Adams *et al.* 2000) identified the precise location of the Roi^{Rev} *P*-element insertion and the *Roi* breakpoint as shown in Figure 4F.

cDNA libraries from eye discs (gift from A. Cowman) and embryos (Zinn *et al.* 1988) were screened with probes from 36A and 37A, and clones corresponding to gene *BG:DS02780.1* and gene *CG15160*, respectively, were recovered and partially sequenced. The 36A inversion breakpoint was found to lie within the first intron of *BG:DS02780.1*, and the 37A breakpoint was 21 nucleotides within the last exon (exon 8) of *CG15160*. We attempted to detect a chimeric transcript consisting of the first exon of *BG:DS02780.1* and the last exon of *CG15160* by reverse transcription (RT)-PCR analysis. To detect transcription from *BG:DS02780.1*, we used a sense primer from the first exon (36A1: 5′ CGCTCTCCTTTTTCATTTCGAAT GCG 3′) and an antisense primer from the second exon (36A2: 5′ CCCCTGGCATCGAATATGCTACAGC 3′). To detect transcription from *CG15160*, we used a sense primer from the seventh exon (37A1: 5′ CGTGGACGCCGCTGGACTCTAGCC 3′) and an antisense primer from the eighth exon (37A2: 5′ GCCCTGGTCCGGGTCCATCAAATCCCGG 3′). Each set of primers yielded the expected size fragments (375 bp for the 36A1–2 pair, 1000 bp for the 37A1–2 pair) when used against poly(A)$^+$ RNA extracted from either wild-type or *Roi*/+ larvae. However, under the same conditions, the combination of primer 36A1 with primer 37A2 did not yield any product of the size expected from the chimeric transcript (500 bp). We concluded that the chimeric gene formed by the *Roi* inversion was not expressed.

Overexpression of *amos*: We first attempted to drive the *UAS-amos* transgene using *Gal4* driver lines with specific expression patterns in the eye. These included h^{H10}, which carries a *P[Gal4]* insertion at the *hairy* locus that is highly expressed anterior to the MF (Huang and Fischer-Vize 1996), a *dac*-Gal4 line that reproduces the *dac* expresssion pattern around the MF (Heanue *et al.* 1999), and a *dpp-Gal4* construct expressed in the MF (Staehling-Hampton *et al.* 1994). All of them led to lethality prior to third larval instar when driving *UAS-amos*, which made it impossible to study their effect on eye patterning. When *UAS-amos* was driven by *GMR-Gal4*, a construct that is expressed behind the MF (Freeman 1996), the flies lived but had no eye defect. We next turned to *hs-Gal4* to express *amos* ubiquitously in third instar larvae. Flies carrying the *hs-GAL4* construct were crossed to flies carrying the *UAS-amos* construct. The progeny were raised at 25° and subjected to a 30-min 37° heat shock at the beginning of third larval instar. Eye discs were dissected out of larvae 24 hr later and stained with antibodies.

Histochemistry: Antibody detection, β-galactosidase activity staining, and retinal sections were performed as previously described (Chanut *et al.* 2000). The rat-anti-ELAV antibody was a gift of G. Rubin and was used at a 1:5 dilution. The mouse-anti-Boss antibody was a gift from L. Zipursky and was used at a 1:1000 dilution. The rabbit-anti-Ato antibody was a gift from Y. N. Jan and was used at a 1:5000 dilution. The

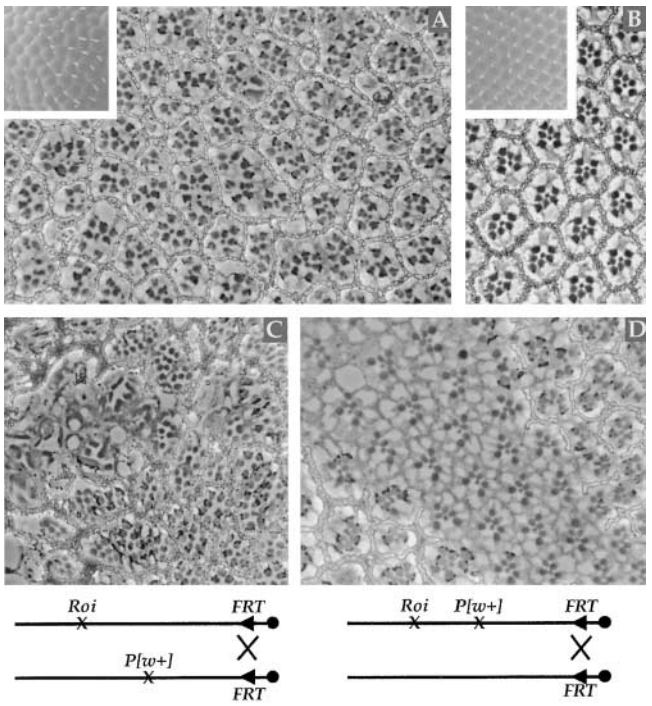

FIGURE 1.—The *Roi* phenotype in the adult retina. Tangential sections of the retina of *Roi* heterozygotes (A) and wild-type (B) adults are shown. Insets show scanning electron microscopy images of the adult eye surface. (C and D) Tangential sections through clones of homozygous *Roi* (C) or homozygous wild-type (D) tissue. The clones are marked with a mutation in the *white* (*w*) gene, which leads to the absence of pigmentation in the pigment cells that surround each photoreceptor cluster and along the photoreceptor rhabdomeres. The diagram at the bottom illustrates the strategy used to mark each clone. (C) In homozygous *Roi* mutant tissue, the retina is more severely disrupted than in heterozygous tissue, and the rhabdomere morphology is very abnormal, but ommatidial clustering is still evident. (D) *Roi* acts locally: Wild-type tissue surrounded by *Roi*/+ tissue differentiates a normal array of ommatidia. At the clone's boundaries, abnormal ommatidia often contain a wild-type (unpigmented) inner photoreceptor.

rabbit-anti-Amos antibody, which will be described elsewhere (P. ZUR LAGE and A. P. JARMAN, unpublished results), was used at a 1:5000 dilution.

RESULTS

***Roi* causes local disruption of the ommatidial lattice:** As previously described (RENFRANZ and BENZER 1989) tangential sections of adult retina show a severe disruption of the ommatidial lattice in *Roi* heterozygotes compared to wild type (Figure 1, A and B). Ommatidia with either more or less than the normal complement of photoreceptors are observed: For instance, the small rhabdomeres characteristic of inner photoreceptors R8 or R7 cells are missing in some ommatidia and clustered in others. Pigment cells are often missing, leading to large photoreceptor clusters that encompass the equivalent of two to three normal ommatidia. The homozygous *Roi* phenotype was assessed in somatic clones (Figure 1C). Homozygous mutant clones were smaller than their wild-type twin spots and contained very aberrant photoreceptors with fused or distorted rhabdomeres (Figure 1C).

To determine whether *Roi* disrupts ommatidial organization locally or at a distance, we generated marked homozygous wild-type clones in a *Roi* heterozygous background (Figure 1D). We found that the wild-type tissue organized into a regular array of normally structured ommatidia, while the surrounding mutant tissue developed into aberrant ommatidia. We conclude that the effect of *Roi* on ommatidial structure and organization is primarily local, though not necessarily cell autonomous. At the edges of the wild-type clones, ommatidia containing mutant and wild-type photoreceptors were usually abnormally structured. Ommatidial structure did not seem to correlate with the genotype of any given photoreceptor; in particular, the presence of a wild-type R8 did not guarantee the formation of normally patterned clusters.

***Roi* increases *hh* and *dpp* expression and disrupts the spacing of R8 precursors:** Because *Roi* suppresses furrow-stop mutations, we were interested in its potential effect on events occurring in the MF. Our marker of the MF, a reporter construct that places β-galactosidase under the control of a disc-specific *decapentaplegic* (*dpp*) enhancer (*dpp-lacZ*; BLACKMAN *et al.* 1991), displayed a broadened expression domain in *Roi* relative to wild type, suggesting an expansion of MF cell fates (Figure 2, A and B). As Dpp signaling in the MF is known to regulate the cell cycle and, indirectly, the shape of cells (PENTON *et al.* 1997; HORSFIELD *et al.* 1998), the expansion of *dpp* expression may contribute in part to the cell shape anomalies that had previously been detected in the MF of *Roi* mutants using antibodies to cell surface markers (RENFRANZ and BENZER 1989).

In wild type, the expression of the *dpp-lacZ* reporter is activated by Hh, which is secreted by cells differentiating behind the MF (HEBERLEIN *et al.* 1993; MA *et al.* 1993). Expression of a *hh-lacZ* reporter construct that monitors faithfully *hh* transcription in discs (LEE *et al.* 1992; MA *et al.* 1993) was also greatly increased behind the MF in *Roi* mutants compared to wild type (Figure 2, C and D). We conclude that *hh* expression is increased in *Roi* mutants, leading to an expansion of MF cell fates as monitored by *dpp-lacZ* expression.

Expression of *ato*, another target of *hh* signaling in the MF (DOMÍNGUEZ and HAFEN 1997; STRUTT and MLODZIK 1997; BOROD and HEBERLEIN 1998), was not markedly increased in *Roi* heterozygotes relative to wild type (Figure 2, E and F). However, *ato*-expressing cells emerged from the MF of *Roi* mutant discs at irregular intervals and often remained in clusters of two or three cells (arrow in Figure 2F) instead of resolving to single evenly spaced cells as in wild type (Figure 2E). The irregular spacing and occasional twinning of the R8 precursors in *Roi* were maintained through later developmental stages, as shown by staining with an antibody against the R8-

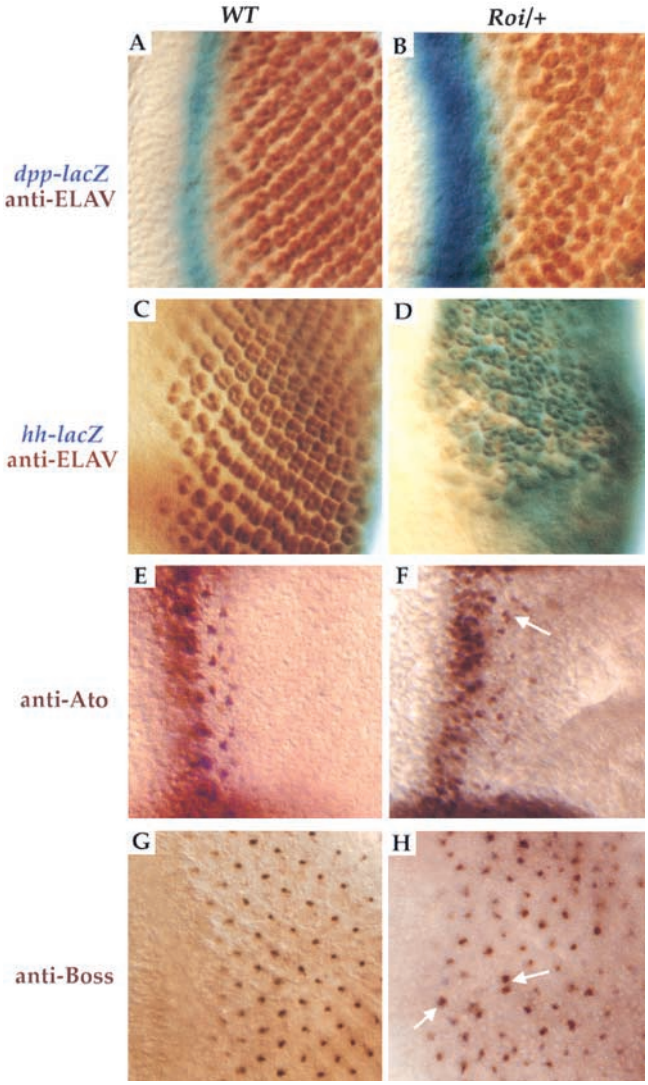

Figure 2.—The *Roi* phenotype in eye discs. Eye imaginal discs from third instar larvae carrying a *dpp-lacZ* (A and B) or *hh-lacZ* (C and D) reporter construct were stained for β-galactosidase activity (blue) and for expression (brown) of the neuronal marker ELAV (A–D), the proneural protein Ato (E and F), and the R8-specific cell-surface marker Boss (G and H). In A–H, posterior is to the right, anterior to the left. (A and B) Expression of the MF marker *dpp-lacZ* (blue) is increased in *Roi* relative to wild type. (C and D) Expression of *hh-LacZ* is increased relative to wild type in differentiating *Roi*/+ clusters. The progressive growth of ommatidial clusters is highly disorganized in *Roi* compared to wild type. (E and F) Single Ato-expressing cells distribute unevenly behind the MF in *Roi* heterozygotes (F) and are often clustered (arrow). (G and H) Expression of Boss confirms the uneven distribution and clustering (arrows) of R8 precursors in the mutant relative to wild type.

specific cell surface protein Bride of Sevenless (Boss; Cagan *et al.* 1992). In wild type, the Boss antigen appears several rows behind the MF as a regular lattice of fine spots (Figure 2G), each of which corresponds to the constricted apical surface of a single R8 cell (Krämer *et al.* 1991; Cagan *et al.* 1992). In contrast, spacing between Boss-expressing cells was irregular in *Roi* heterozygotes (Figure 2H), and larger spots, consistent with clusters of two to three cells, were frequent. This suggests that *Roi* interferes with the early patterning events that allow the precise spacing of individual R8 precursors.

Irregular R8 selection was accompanied with the disorganized recruitment of other ommatidial cells, as shown in discs stained with an antibody against the pan-neural marker ELAV (Robinow and White 1991). In wild type, the progressive induction of photoreceptor differentiation by the R8 founder follows a strict temporal and spatial sequence and creates a smooth gradient of ommatidial maturation, with clear polarity along the anteroposterior axis (Tomlinson and Ready 1987a,b). In *Roi*, while a maturation gradient was still evident behind the MF, the recruitment of photoreceptors did not appear to follow a stereotyped pattern (Figure 2, B and D). Whether this is a direct effect of the *Roi* mutation or an indirect consequence of abnormal R8 spacing is not known. In summary, our data demonstrate that *Roi* affects retinal patterning within the MF, at the level of R8 formation, and potentially behind the MF, at the level of further photoreceptor recruitment.

Mutations in *da* and *hh* act as strong suppressors of the *Roi* phenotype: While *Roi* suppresses the stop-furrow phenotype of ro^{Dom} (Figure 3, A and B) and hh^{bar3} (Heberlein *et al.* 1993), it is itself modified by mutations in several genes known to affect eye differentiation or furrow progression. For instance, removing one copy of *hh* led to a noticeable suppression of eye roughness in *Roi* heterozygotes. In a tangential section (Figure 3C), the retina still appeared somewhat disorganized, but at least 50% of the ommatidia had regained a normal structure and orientation (Figure 3C, arrows).

The strongest suppression of the rough eye phenotype was achieved with the removal of one copy of *da*. In section, the retina appeared almost normal (compare Figure 3D with Figure 1B), with only an occasional abnormally structured ommatidium. *da* encodes a protein of the bHLH family (Caudy *et al.* 1988) that is required for Ato's proneural function in the eye (Brown *et al.* 1996). Interestingly, removal of one copy of *ato* had no detectable impact on the *Roi* phenotype (not shown), while simultaneous removal of *ato* and *da* only slightly improved the suppression of patterning defects relative to the removal of *da* alone (Figure 3E).

Molecular analysis of the 36A–37A region: On the basis of its failure to complement the lethality of specific chromosomal deficiencies, *Roi* had previously been mapped to the 36F7–37B8 region (Voelker and Langley 1978). Deficiencies spanning this region do not lead to eye roughness, suggesting that *Roi* is a gain-of-function mutation. To identify the *Roi* gene, we obtained revertants of the rough eye phenotype by mutagenizing a *Cyo, Roi* chromosome using X-ray irradiation or by *P*-element-mediated dysgenesis (see materials and methods). Several X-ray-induced revertants showed cytological ab-

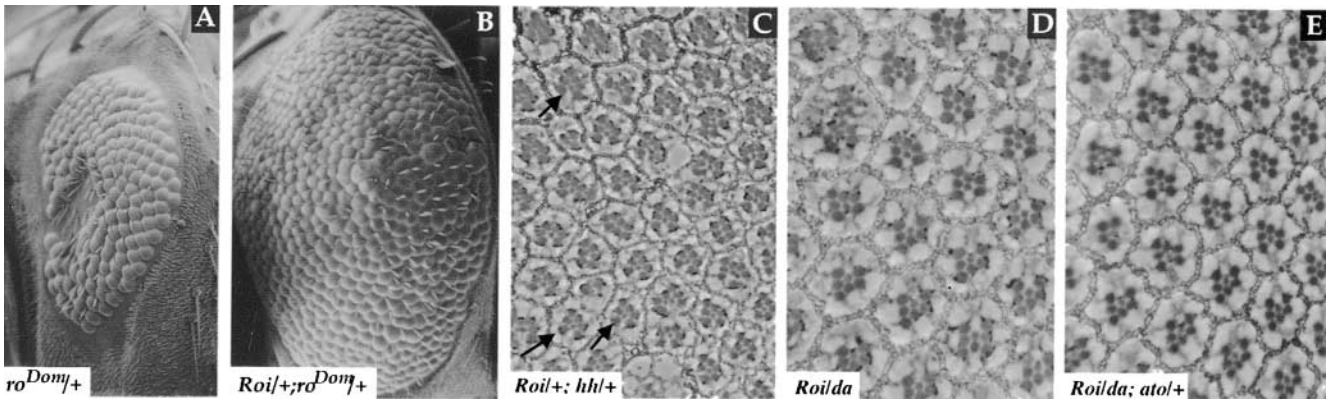

FIGURE 3.—Genetic interactions between *Roi* and mutations that affect retinal differentiation. (A and B) Scanning electron microscopy images of the eye of a ro^{Dom} heterozygote (A) and a *Roi*, ro^{Dom} double heterozygote (B). (C–E) Tangential sections of adult retinae from flies heterozygous for *Roi* and strong alleles of *hh* (C, hh^{13c}), *da* (D, da^{UX}), and *ato* combined with *da* (E, ato^{1}, da^{UX}).

normalities in the 36–37 region (not shown), confirming the initial mapping of *Roi*. One of the *P*-induced potential revertants, Roi^{Rev}, contained a *P* element at 37A and was retained for further analysis. In retinal sections, Roi^{Rev} ommatidial structure and patterning appeared indistinguishable from wild type (Figure 4A; compare with Figure 1B). In discs, staining for Ato and Boss expression confirmed that spacing and resolution of R8 precursors was normal (Figure 4, B and C; compare with Figure 2, E and G). In addition to reverting to wild-type eye morphology, Roi^{Rev} had also lost most of its ability to suppress the furrow-stop phenotype of ro^{Dom} (Figure 4D; compare with Figure 3, A and B) and hh^{bar3} (not shown). Furthermore, excision of the *P* element at 37A restored the *Roi* phenotype (see MATERIALS AND METHODS). Taken together, these observations confirmed that *Roi* is a gain-of-function mutation that can be reverted by the inactivation of a gene located at 37A.

To identify this gene, genomic DNA flanking the insertion was obtained from a phage library of Roi^{Rev} genomic DNA (see MATERIALS AND METHODS). Phages that contained the *P* element at 37A were found to hybridize to two locations on wild-type polytene chromosomes: 37A and 36A. Two sites of hybridization were also seen when wild-type genomic DNA from the 37A region was hybridized to *Roi* or Roi^{Rev} polytenes. This indicated that *Roi* and Roi^{Rev} carried an inversion between 36A and 37A. This inversion may have gone unnoticed in previous cytological examinations of *CyO, Roi* chromosomes because of the abnormal conformation frequently adopted by polytene chromosomes in the 36–39 region (LINDSLEY and ZIMM 1992).

DNA sequence analysis of the Roi^{Rev} phage clones and of wild-type genomic clones obtained from the 36A and 37A regions identified the location of the inversion breakpoints in *Roi* and showed that the *P* element in Roi^{Rev} had inserted 8.4 kb distal to the 37A breakpoint, inside the inversion (Figure 4E). cDNA clones homologous to the 36A and 37A region were isolated from wild-type eye disc and embryonic libraries and shown by cytology and molecular analysis to span the *Roi* inversion breakpoint. Sequence comparisons revealed that the *P* element in Roi^{Rev} lay 14 bp upstream of the first exon of a gene of unknown function normally located at 36A, later identified as *BG:DS02780.1* (ASHBURNER *et al.* 1999). The inversion breaks in the first intron of the 36A gene and within the last exon of a gene of unknown function normally located at 37A, later identified as *CG15160* (ADAMS *et al.* 2000). We first hypothesized that a chimeric gene formed by the 3′ portion of the 37A gene (*CG15160*) under the control of the 5′ portion of the 36A gene (*BG:DS02780.1*) was responsible for the *Roi* phenotype. In Roi^{Rev}, expression of this gene would be abolished by the *P* insertion in the promoter region of *BG:DS02780.1*. However, we could not detect the expression of a chimeric RNA by RT-PCR in *Roi* heterozygotes (see MATERIALS AND METHODS), and this hypothesis was abandoned.

Later releases of the Drosophila genome sequence in the 36–37 area revealed other potential candidates for the *Roi* gene (Figure 4E). The *BG:DS02780.1* gene was found to overlap a three-gene cluster encoding imaginal disc growth factors (IDGF1–3) related to Chitinase (KAWAMURA *et al.* 1999). In *Roi*, the 5′ end of the *Idgf* gene cluster is located 5.3 kb away from the inversion breakpoint. The first exon of *BG:DS02780.1* lies within the first intron of *Idgf2*, on the opposite strand. Consequently, the Roi^{Rev} *P* element is also inserted within *Idgf2*'s first intron. The *Idgf* gene cluster, ~8 kb long, lies 12.3 kb downstream of *dachshund* (*dac*), which encodes a transcription factor implicated in eye morphogenesis (MARDON *et al.* 1994). Outside the inversion, 2.6 kb proximal to the 37A breakpoint is *amos*, a proneural gene required for the development of olfactory organs (GOULDING *et al.* 2000; HUANG *et al.* 2000).

***Roi* causes misexpression of *amos* in the eye disc:** Of the genes mapping near the genomic breakpoint in *Roi*, *dac* and *amos* appeared as the most likely candidates to

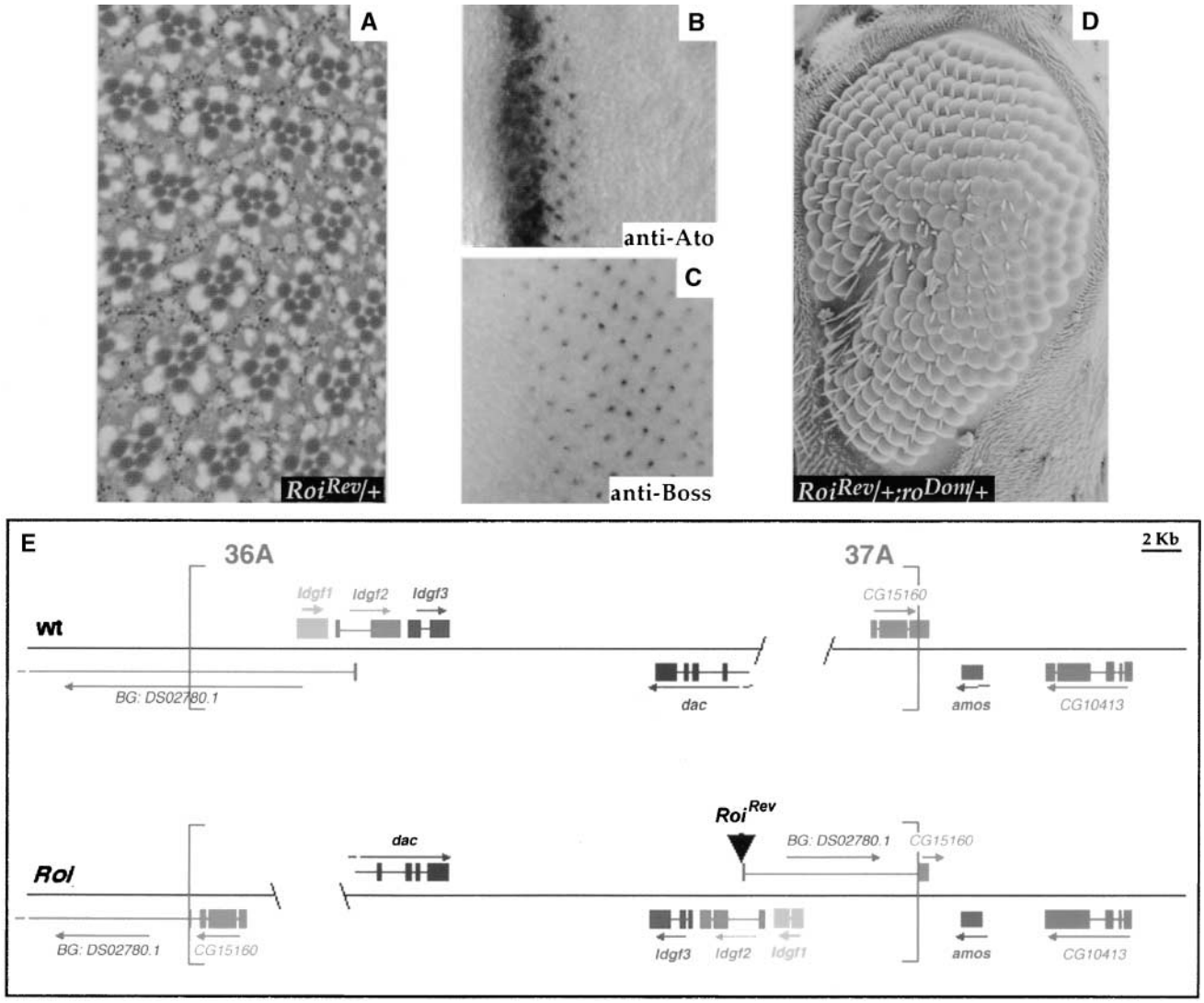

FIGURE 4.—A revertant of the *Roi* phenotype maps close to *amos*. (A) Tangential section through the retina of a *w*; Roi^{Rev}/+ adult. (B and C) Antibody staining of third instar eye imaginal discs to reveal Ato (B) and Boss (C) expression. (D) Scanning electron microscopy image of the eye of an adult heterozygous for Roi^{Rev} and ro^{Dom}. (E) Genomic map of the 36A–37A region in wild type and *Roi*. The distance from the *P* element to the inversion breakpoint was inferred from sequence comparison with genomic P1 clone DS02780. The location of all genes indicated on the map is inferred from the BDGP/Celera genomic sequence release (ADAMS *et al.* 2000; RUBIN *et al.* 2000).

disrupt retinal development in *Roi*. *dac* belongs to a network of genes including *eyeless*, *eyes absent*, and *sine oculis* that imparts retinal fate to the cells of the eye epithelium (CHEN *et al.* 1997; PIGNONI *et al.* 1997). *amos* is a proneural gene most closely related to *ato* (JARMAN *et al.* 1993)—the two genes share 74% sequence identity over their entire bHLH region—that has been reported to mimic *ato* in the induction of sense organs in embryos and adults (GOULDING *et al.* 2000; HUANG *et al.* 2000).

Staining with an antibody directed against the Dac protein failed to detect any difference among *Roi*, Roi^{Rev}, and wild-type eye discs (Figure 5, A–C). In addition, *Roi* complemented lethal *dac* alleles and the rough-eye phenotype was insensitive to a reduction in *dac* gene dosage (not shown); the revertant also complemented lethal and eye-specific *dac* alleles (not shown). We conclude that *dac* is not affected by the *Roi* inversion and not implicated in the resulting rough-eye phenotype. In contrast, *amos* expression was markedly different between *Roi* and wild type (Figure 5, D and E). In wild type, *amos* expression does not begin in the eye-antennal region until pupal stages and remains confined to the area giving rise to olfactory sensilla precursors in the antenna (GOULDING *et al.* 2000). In *Roi* mutant discs from third instar larvae, we found high levels of Amos protein in a broad area surrounding the MF (Figure 5E). Ectopic expression was sharply reduced in Roi^{Rev} discs (Figure 5F), although not completely abolished, which might explain that Roi^{Rev} retains some ability to suppress ro^{Dom} (Figure 4D). Together, these data suggested that

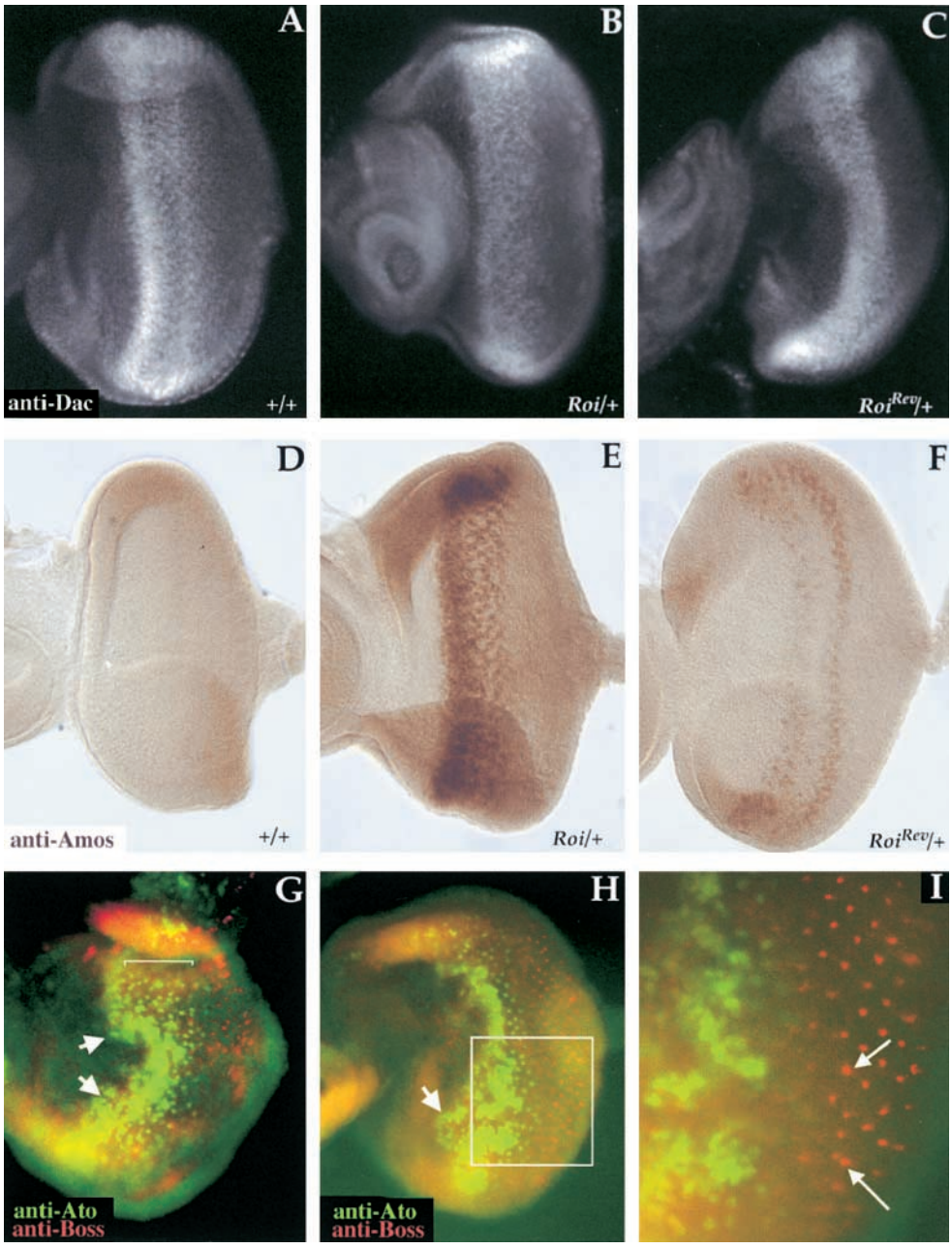

FIGURE 5.—The *Roi* phenotype results from ectopic expression of *amos* in the eye disc. (A–F) Staining of wild-type (A and D), *Roi*/+ (B and E), and Roi^{Rev}/+ (C and F) third instar eye-antennal discs with an antibody against the retinal specification protein Dachshund (A–C) or the proneural protein Amos (D–F). (G–I) Overexpression of *amos* leads to R8 patterning defects. *amos* was ubiquitously expressed in third instar larvae using a *UAS-amos* construct under the control of a *hs-GAL4* construct. Third instar eye discs were stained with antibodies against Ato (green) and Boss (red). (G and H) Ubiquitous *amos* causes an expansion of the front of *ato* expression, associated with frequent bulges (white arrows) and the prolonged expression of *ato* in isolated cells behind the MF (bracket). (I) Close-up of the area highlighted in (H). Staining for Boss expression reveals irregular spacing and clustering of R8 cells (arrows).

the *Roi* phenotype might result from ectopic expression of the proneural gene *amos* in the eye disc.

To test this hypothesis, we attempted to drive a *UAS-amos* transgene under the control of *GAL4* constructs expressed in the MF or anterior to it. However, *amos* misexpression under all the drivers tested caused early larval lethality (see MATERIALS AND METHODS), making it impossible to study an effect in third instar eye discs. We therefore expressed *amos* ubiquitously in a short pulse during the third larval stage using a *hs-Gal4* driver (see MATERIALS AND METHODS). This allowed survival to adult stages and led to a roughening of the adults' eye surface (not shown). In discs, *amos* overexpression led to an expansion of *ato* expression (Figure 5, G and H): Instead of the sharp band of Ato protein observed ahead of wild-type furrows (see Figure 2E), the front of differentiation was marked by an irregular and mottled zone of *ato* expression. Forward bulges of the Ato front (arrows in Figure 5, G and H) suggested regions of accelerated furrow progression, without proper patterning. Behind this expanded front of Ato protein, single Ato-expressing cells were found over a broader area than in wild type (bracket in Figure 5G), suggesting that *ato* expression persisted longer in the R8 precursors than in wild type. In addition, spacing of these cells was often irregular. Staining for Boss expression confirmed the presence of irregularly spaced R8 precursors and of occasional R8 clusters (Figure 5I).

In summary, overexpression of *amos* in eye discs under heat-shock control leads to defects in R8 patterning that are similar to those observed in *Roi* mutant discs, which is consistent with the proposal that the *Roi* phenotype is

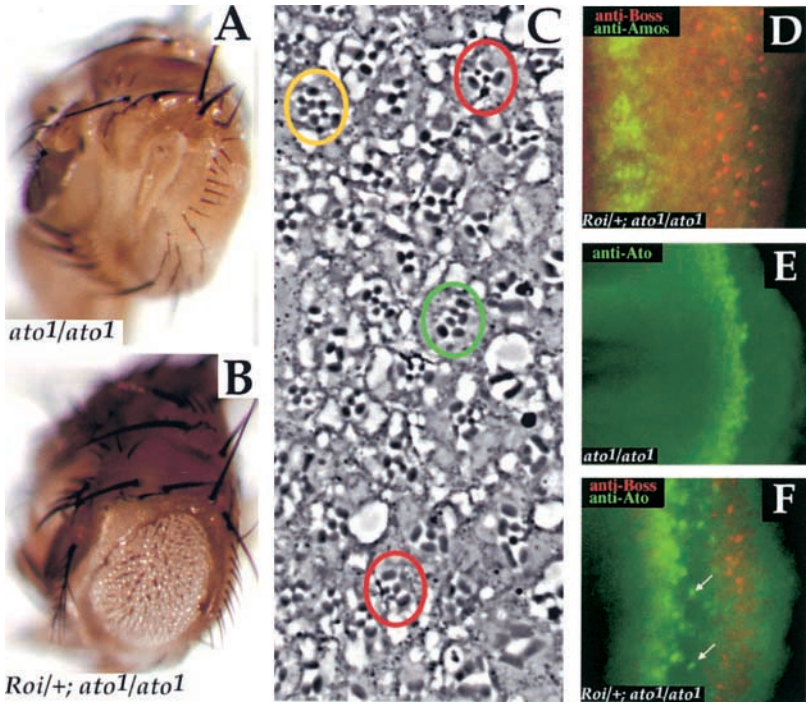

FIGURE 6.—*Roi* restores retinal differentiation in ato^1 homozygotes. (A and B) Photographs of adult heads from ato^1/ato^1 (A) or *Roi*/+; ato^1/ato^1 (B) adults. (C) Tangential retinal section of a *Roi*/+; ato^1/ato^1 double mutant. Ommatidia are disorganized and may contain an excess of photoreceptors (yellow circle), an excess of inner photoreceptors (red circles), or a lack of inner photoreceptors (green circle). (D–F) Third instar imaginal discs from ato^1 homozygotes (E) or *Roi*/+; ato^1/ato^1 (D and F) stained to reveal expression of Amos (green, D), Ato (green, E and F) and Boss (red, D and F). (D) *Roi* causes Amos misexpression (green) and restores the formation of Boss-expressing (red) R8 cells in ato^1 homozygotes. (E) ato^1 homozygotes express a mutant Ato protein that fails to resolve to single cells. (F) *Roi* restores the resolution of Ato to isolated cells (arrows) behind the MF in ato^1 homozygotes.

caused by misexpression of *amos* in the eye. On the other hand, heat-shock-driven misexpression of *amos* also causes a considerable expansion or stabilization of *ato* expression relative to wild type, an effect that was not observed in *Roi*. This discrepancy might simply reflect the different patterns of *amos* misexpression in the two situations: In *Roi*, *amos* expression is confined to a portion of the eye disc near the MF, whereas it is ubiquitous under heat-shock control. While we cannot eliminate the possibility that other genes in the vicinity of the *Roi* breakpoints participate in the *Roi* phenotype, we conclude that the effect of *Roi* on *ato* patterning is due mainly to ectopic expression of *amos* in the retinal portion of the eye-antennal disc.

***Roi* suppresses the differentiation defect of ato^1 homozygotes:** Because *amos* and *ato* encode related bHLH proteins with somewhat overlapping specificity in the differentiation of sense organs (GOULDING *et al.* 2000; HUANG *et al.* 2000), we were curious to see whether *amos* could assume some of *ato*'s functions in retinal differentiation. We introduced the *Roi* mutation in the background of the ato^1 mutation, a viable, recessive loss-of-function *ato* allele that does not allow the development of R8 photoreceptors (JARMAN *et al.* 1994). While the eyes of ato^1 homozygotes are reduced to a slit of pigment cells (Figure 6A), the presence of one copy of *Roi* allows them to reach one-third to one-half of wild-type size (Figure 6B). Upon sectioning, ommatidial clusters appeared disorganized and composed of an abnormal number of photoreceptors whose rhabdomeres were often elongated and misshapen (Figure 6C). In many ommatidia, however, we were able to discern smaller rhabdomeres (Figure 6C, red circles), suggesting the presence of R8 photoreceptors. To confirm the identity of these cells, we stained imaginal discs from double mutant (*Roi*/+; ato^1) larvae with the anti-Boss antibody. The Boss protein was detectable as small spots in a disorganized array, but at distances comparable to those observed between R8 precursors in wild type (Figure 6D). This suggested that most, if not all, of the ommatidial clusters that developed in this double mutant background contained a Boss-expressing, presumed R8 cell.

The ato^1 allele expresses a mutant protein that is recognized by the anti-Ato antibody and forms a continuous band near the posterior disc margin that fails to resolve to single cells in ato^1 homozygotes (Figure 6E; SUN *et al.* 1998). In the presence of *Roi*, however, resolution to single cells was clearly restored behind the continuous front of *ato* expression (Figure 6F, arrows). The distribution of these cells was uneven and they occasionally remained clustered, in a manner reminiscent of *Roi*'s effect in an otherwise wild-type background (compare Figure 6F with Figure 2F). This shows that *Roi* can restore the resolution of the mutant Ato protein to isolated cells, as well as allowing the adoption of the R8 cell fate, as monitored by Boss expression. Whether the Boss-expressing cells observed in the *Roi*; ato^1 double mutant derive from the single *ato*-expressing cells that emerge from the MF could not be ascertained, because *ato* expression subsides several rows before the appearance of Boss (Figure 6F).

DISCUSSION

***Roi* is a gain-of-function allele of *amos*:** Several observations suggest that *Roi* is a gain-of-function allele of *amos*. First, the Amos protein is abundantly expressed in the eye imaginal discs of *Roi* heterozygotes, whereas it is never

detected at this location in wild-type eye-antennal discs. Second, reversion of the *Roi* phenotype is achieved by a *P*-element insertion a few kilobases downstream of *amos* and is associated with the severe reduction of *amos* expression in the eye. Third, overexpression of *amos* in wild type, under heat-shock control, causes the disruption of R8 cells spacing in a manner very reminiscent of *Roi*. Fourth, the *Roi* phenotype is almost completely suppressed by mutations in *daughterless*, a gene that encodes a bHLH protein shown to form heterodimers *in vitro* with the Amos protein (Huang *et al.* 2000). Together, these observations constitute strong evidence that the *Roi* phenotype is due to the ectopic expression of the bHLH protein Amos.

The basis of *amos*'s misexpression in *Roi* is unclear. The 36A–37A chromosomal inversion that we mapped in *Roi* breaks 2.6 kb downstream of *amos* and brings it in the vicinity of the *Idgf* gene cluster (7.9 kb away) and of *dac* (29.1 kb away). The inversion appears to remove a 3′ endogenous enhancer of *amos*, as *Roi* behaves as a loss-of-function *amos* allele in the development of antennal olfactory sense organs (P. zur Lage and A. P. Jarman, unpublished results). In the absence of endogenous regulatory sequences, *amos* may respond to other neighboring enhancers. Whether the genes brought closest to *amos* in *Roi*—the *Idgf* gene cluster and the 5′-most portion of *BG:DS02780.1* gene—have enhancers that can direct gene expression in the eye is at present unknown. At this point, the most likely source of an eye-specific enhancer is *dac*, in spite of its distance from *amos* (29 kb), since its domain of expression in the eye coincides roughly with that of *amos* in *Roi* (Mardon *et al.* 1994; Figure 5, A, B, and E).

Genes other than *amos* may be affected by the inversion and contribute to some extent to the *Roi* phenotype. Our experiments eliminated the possibility that *dac*, a likely candidate considering its normal involvement in eye differentiation (Mardon *et al.* 1994; Chen *et al.* 1997), had a part in the *Roi* phenotype. We also do not believe that a chimeric gene straddling the 37A breakpoint participates in the *Roi* phenotype because this gene, made of a noncoding exon from the *BG:DS07820.1* gene and a portion of the last exon of the *CG15160* gene, is probably not coding. In addition, its expression was undetectable in *Roi* mutants. No mutation has been reported in the *Idgf* genes or in the putative genes immediately proximal to *amos*, and whether they contribute to the *Roi* phenotype cannot be ascertained. For the sake of simplicity, the rest of our discussion assumes that *amos* misexpression in the eye disc mediates all aspects of the *Roi* phenotype, unless otherwise mentioned.

Amos activates *ato* expression: We find that *Roi* disrupts the patterning of the *ato*-expressing cells that emerge from the posterior edge of the furrow: Their distribution is irregular and they often subsist as small clusters of two or three cells, instead of resolving to evenly distributed single cells. This indicates that intermediate clusters distribute unevenly along the MF and fail to resolve properly to single R8 cell precursors. While the formation and distribution of intermediate groups depends mostly on *Notch*-mediated lateral inhibition (Cagan and Ready 1989; Baker and Zitron 1995; Baker *et al.* 1996), the resolution of *ato* expression to single R8 precursors requires the repression of *ato* expression by the homeobox gene *ro* (Dokuçu *et al.* 1996). In the absence of *ro* function, *ato* expression is maintained in clusters of two to three cells known as the R8 equivalence group, which leads to the differentiation of additional R8 cells. Our data suggest that *amos* interferes both with lateral inhibition and with the inhibitory effect of *ro* on *ato* expression. The expression of a *ro-lacZ* reporter construct (Heberlein *et al.* 1991) is not detectably repressed at the posterior edge of the MF in the background of the *Roi* mutation (F. Chanut and U. Heberlein, unpublished observation). We therefore do not believe that ectopic *amos* can prevent *ro* expression. It remains possible, however, that, in *Roi*, Amos somehow prevents the Rough protein from repressing *ato*. Antagonism between Amos and Ro could explain why *Roi* is a strong suppressor of the ro^{Dom} stop-furrow phenotype, which is caused by ectopic *ro* expression anterior to the MF (Chanut *et al.* 2000).

Ubiquitous expression of *amos* under a heat-shock promoter gives rise to similar defects in the patterning of *ato*-expressing cells behind the MF as *Roi*, including the irregular distribution and frequent twinning of R8 precursors. In addition, there is considerable expansion of the domain of *ato* expression, both anterior and posterior to the MF, which suggests that Amos can, directly or indirectly, activate *ato* expression. Inhibitors of *ato* expression anterior to the MF include the HLH proteins Hairy and Emc (Brown *et al.* 1995) and Hairless (Chanut *et al.* 2000). It is possible that Amos interferes with their expression or with their activity (for instance, an excess of Amos protein might titrate out the repressor EMC). Alternatively, because of its high sequence similarity to Ato, Amos might directly activate *ato* expression, mimicking Ato's ability to autoregulate (Sun *et al.* 1998). This would also explain why ectopic expression of *amos* causes the prolonged expression of *ato* in the R8 precursors, where *ato* maintenance is due primarily to autoregulation (Sun *et al.* 1998). As precocious or excessive *ato* expression is known to lead to aberrant *ato* patterning (Brown *et al.* 1995; Dokuçu *et al.* 1996), the patterning defects observed upon Amos overexpression could at least in part be explained by *ato* upregulation.

In conclusion, we propose that ectopic expression of Amos leads to inappropriate *ato* expression, either by directly activating *ato* or by interfering with repressors of *ato* expression. In *Roi*, the effect of Amos is milder—in particular, *ato* expression levels were not detectably elevated in the MF—presumably because *amos* misexpression is weaker and spatially more restricted than when *amos* is overexpressed ubiquitously. We note that a slight increase of *ato* expression in *Roi* could also explain the

strong suppression of the ro^{Dom} stop-furrow phenotype, since ro^{Dom} is efficiently suppressed by heterozygous mutations in *groucho* and *Hairless*, which presumably lead only to slight elevations of *ato* levels (Chanut *et al.* 2000).

***Roi* patterning defects are suppressed by mutations in *hedgehog* (*hh*) and *daughterless* (*da*):** Regularity and proper polarization of the ommatidial lattice are almost completely restored in *Roi* mutant eyes by a reduction of the *da* gene dosage and partially restored by a reduction of the *hh* gene dosage. Since Amos and Da have been shown to form heterodimers *in vitro* (Huang *et al.* 2000), the strong sensitivity to *da* gene dosage suggests that all the effects of the Amos protein in *Roi* eyes are carried out by Amos-Da heterodimers. The sensitivity to *hh* gene dosage is intriguing because *hh* is upregulated behind the MF in *Roi* discs. This observation suggests that excess *hh* might contribute to eye roughness. Overexpression of *hh* behind the MF does not usually result in R8 patterning defects (White and Jarman 2000; F. Chanut and U. Heberlein, unpublished observations), although in a genetic background where R8 spacing is already compromised, it can further enhance the failure to resolve *ato* expression to single R8 cells (White and Jarman 2000). It is therefore possible that the excess Hh produced in *Roi* mutants exacerbates the effect of Amos on R8 patterning. Removing one copy of the *hh* gene would alleviate this effect and partially suppress eye roughness.

Why *hh* is overexpressed in *Roi* mutants is unclear. In wild type, expression of *hh* behind the MF is limited to the R2 and R5 precursors and requires the Da protein (Brown *et al.* 1996). In *Roi*, the formation of ectopic Da-Amos heterodimers might activate *hh* expression in more cells than in wild type. In this case, *da* mutations would affect the *Roi* phenotype at two levels: in the MF, by reducing *amos*'s interference with *ato* patterning, and behind the MF, by reducing *hh* expression. This could explain the strong suppression of *Roi* by halving the *da* gene dosage. At this point, however, it remains also possible that the increased transcription of *hh* in *Roi* results from the misexpression of other genes in the vicinity of the *Roi* inversion breakpoints. Regardless of its cause, increased *hh* expression behind the MF is likely to explain why *Roi* suppresses the furrow-stop phenotype of the hypomorphic allele hh^{bar3}, which is thought to cause an eye-specific transcriptional defect (Lee *et al.* 1992; Huang and Kunes 1996). We propose that *Roi* overcomes the transcriptional block of hh^{bar3}, which in turn restores Hh production to sufficient levels for normal MF progression.

Can *amos* induce photoreceptor differentiation? It has recently been shown that ectopic expression of the proneural gene *scute* (*sc*) in ato^{1} homozygotes can lead to the differentiation of photoreceptors in the apparent absence of R8 founders (Sun *et al.* 2000). We similarly tested whether *amos* could induce photoreceptor differentiation in the absence of *ato* function by introducing *Roi* in the background of ato^{1} homozygotes. We found that this restored retinal differentiation, but that, in contrast to *sc* overexpression, it was accompanied by the restoration of R8 cells. In addition, whereas in ato^{1} mutants the Ato protein fails to become patterned, resolution of *ato* to single cells behind the MF was restored in *Roi*.

This experiment suggests that, in contrast to *sc*, *amos* does not induce the differentiation of photoreceptors independently of an R8 founder. Consistent with this proposal, *Roi* is not associated with an overall excess of outer photoreceptors relative to R8s in a wild-type background (Renfranz and Benzer 1989). In the *Roi*; ato^{1} adult eyes, we do observe a number of photoreceptor clusters devoid of R8 cells (Figure 6C), which could indicate that they were induced directly by *amos*, in the absence of any R8 founder. However, R8 precursor cells are present at high density in double mutant discs (Figure 6D). We therefore find it more likely that all the photoreceptor clusters that form in *Roi*; ato^{1} double mutants were seeded by an R8 founder; some R8 cells may later degenerate, for instance, because of incomplete fate specification.

As for the origin of the R8 cells in the *Roi*; ato^{1} double mutants, we envision two scenarios. In the first one, all R8 cells derive from the isolated *ato*-expressing cells that are restored by *Roi* behind the MF of ato^{1} mutant discs. This implies that ato^{1} is able to support the differentiation of R8 cells, although it carries point mutations that are thought to abolish the Ato protein's DNA-binding activity (Jarman *et al.* 1994). This would suggest that ato^{1} retains some residual activity and becomes potentiated in the *Roi* background, either because its expression is elevated or via synergy with *amos* at the level of *ato*'s transcriptional targets.

In the second and perhaps more likely scenario, *amos*, due to its high similarity with *ato*, directly induces the differentiation of cells with at least some R8 characteristics, including the ability to maintain *ato* expression, to express Boss, and to recruit other photoreceptor cell types. A potential difficulty with this scenario is that the R8 cells that develop in the *Roi*; ato^{1} mutants form a lattice that, though imperfect, is reminiscent of wild type. How do R8 cells become patterned when they are induced by *amos*? We note first that *amos* expression in *Roi*, while continuous ahead of the MF, becomes restricted to groups of cells behind the MF (see Figure 5E). Second, experiments in which *ato* was expressed ubiquitously have shown that only the cells of the R8 equivalence group have the competence to adopt an R8 fate (Dokuçu *et al.* 1996). The combination of restricted cell competence and patterned *amos* expression behind the MF can probably account for the distribution of R8 cells in the *Roi*; ato^{1} double mutant.

In conclusion, we propose that *amos* can promote photoreceptor differentiation in the eye and that its activity is biased toward the induction of the R8 fate,

which it may achieve by substituting for *ato* or by increasing *ato* activity. The *Roi* mutation, a gain-of-function allele that misexpresses *amos* in the eye, provides a promising background in which to identify transcriptional targets of *amos* and *ato*, as well as genes that modulate their activity.

We thank John Tamkun for the use of his cosmid library, Gerry M. Rubin for his support in the initial stages of this project, Dennis Ballinger for sharing information on *Roi* and providing the *isoRoi* stock, the Bloomington Stock Center and various members of the fly community for providing fly stocks, and members of the Heberlein lab, past and present, for their technical and intellectual input. This work was supported by a grant from the National Science Foundation (IBN-9996214) and from the National Institutes of Health (EY-11410) to U.H.

LITERATURE CITED

Adams, M. D., S. E. Celniker, R. A. Holt, C. A. Evans, J. D. Gocayne *et al.*, 2000 The genome sequence of Drosophila melanogaster. Science **287:** 2185–2195.

Albagli, O., M. P. Laget and F. Chanut, 1997 Photoreceptor differentiation in Drosophila: transduction and interpretation of the RTK signaling pathway. Med. Sci. **13:** 184–191.

Ashburner, M., P. Thompson, J. Roote, P. F. Lasko, Y. Grau *et al.*, 1990 The genetics of a small autosomal region of *Drosophila melanogaster* containing the structural gene for alcohol dehydrogenase. Genetics **126:** 679–694.

Ashburner, M., S. Misra, J. Roote, S. E. Lewis, R. Blazej *et al.*, 1999 An exploration of the sequence of a 2.9-Mb region of the genome of *Drosophila melanogaster*: the Adh region. Genetics **153:** 179–219.

Baker, N. E., and G. M. Rubin, 1992 Ellipse mutations in the Drosophila homologue of the EGF receptor affect pattern formation, cell division, and cell death in eye imaginal discs. Dev. Biol. **150:** 381–396.

Baker, N. E., and A. E. Zitron, 1995 Drosophila eye development: Notch and Delta amplify a neurogenic pattern conferred on the morphogenetic furrow by scabrous. Mech. Dev. **49:** 173–189.

Baker, N. E., M. Mlodzik and G. M. Rubin, 1990 Spacing differentiation in the developing Drosophila eye: a fibrinogen-related lateral inhibitor encoded by scabrous. Science **250:** 1370–1377.

Baker, N. E., S. Yu and D. Han, 1996 Evolution of proneural atonal expression during distinct regulatory phases in the developing Drosophila eye. Curr. Biol. **6:** 1290–1301.

Blackman, R. K., R. Grimaila, M. M. Koehler and W. M. Gelbart, 1987 Mobilization of hobo elements residing within the decapentaplegic gene complex: suggestion of a new hybrid dysgenesis system in Drosophila melanogaster. Cell **49:** 497–505.

Blackman, R. K., M. Sanicola, L. A. Raftery, T. Gillevet and W. M. Gelbart, 1991 An extensive 3′ *cis*-regulatory region directs the imaginal disk expression of *decapentaplegic*, a member of the TGF-b family in *Drosophila*. Development **111:** 657–666.

Borod, E. R., and U. Heberlein, 1998 Mutual regulation of decapentaplegic and hedgehog during the initiation of differentiation in the Drosophila retina. Dev. Biol. **197:** 187–197.

Brand, A. H., A. S. Manoukian and N. Perrimon, 1994 Ectopic expression in Drosophila. Methods Cell Biol. **44:** 635–654.

Brennan, C. A., and K. Moses, 2000 Determination of Drosophila photoreceptors: timing is everything. Cell. Mol. Life Sci. **57:** 195–214.

Brown, N. L., C. A. Sattler, S. W. Paddock and S. B. Carroll, 1995 Hairy and emc negatively regulate morphogenetic furrow progression in the Drosophila eye. Cell **80:** 879–887.

Brown, N. L., S. W. Paddock, C. A. Sattler, C. Cronmiller, B. J. Thomas *et al.*, 1996 daughterless is required for Drosophila photoreceptor cell determination, eye morphogenesis, and cell cycle progression. Dev. Biol. **179:** 65–78.

Cagan, R., 1993 Cell fate specification in the developing Drosophila retina. Development (Suppl.): 19–28.

Cagan, R. L., and D. F. Ready, 1989 Notch is required for successive cell decisions in the developing Drosophila retina. Genes Dev. **3:** 1099–1112.

Cagan, R. L., H. Krämer, A. C. Hart and S. L. Zipursky, 1992 The bride of sevenless and sevenless interaction: internalization of a transmembrane ligand. Cell **69:** 393–399.

Caudy, M., H. Vässin, M. Brand, R. Tuma, L. Y. Jan *et al.*, 1988 Daughterless, a Drosophila gene essential for both neurogenesis and sex determination, has sequence similarities to myc and the achaete-scute complex. Cell **55:** 1061–1067.

Chanut, F.. and U. Heberlein, 1997 Role of decapentaplegic in initiation and progression of the morphogenetic furrow in the developing Drosophila retina. Development **124:** 559–567.

Chanut, F., A. Luk and U. Heberlein, 2000 A screen for dominant modifiers of ro^{Dom}, a mutation that disrupts morphogenetic furrow progression in Drosophila, identifies groucho and hairless as regulators of atonal expression. Genetics **156:** 1203–1217.

Chen, R., M. Amoui, Z. Zhang and G. Mardon, 1997 Dachshund and eyes absent proteins form a complex and function synergistically to induce ectopic eye development in Drosophila. Cell **91:** 893–903.

Dokuçu, M. E., S. L. Zipursky and R. L. Cagan, 1996 Atonal, rough and the resolution of proneural clusters in the developing Drosophila retina. Development **122:** 4139–4147.

Domínguez, M., 1999 Dual role for Hedgehog in the regulation of the proneural gene atonal during ommatidia development. Development **126:** 2345–2353.

Domínguez, M., and E. Hafen, 1997 Hedgehog directly controls initiation and propagation of retinal differentiation in the Drosophila eye. Genes Dev. **11:** 3254–3264.

Engels, W. R., 1989 P elements in Drosophila, pp. 437–484 in *Mobile DNA*, edited by D. E. B. a. M. M. Howe. American Society of Microbiology, Washington, DC.

Freeman, M., 1996 Reiterative use of the EGF receptor triggers differentiation of all cell types in the *Drosophila* eye. Cell **87:** 651–660.

Freeman, M., 1997 Cell determination strategies in the *Drosophila* eye. Development **124:** 261–270.

Goulding, S. E., P. zur Lage and A. P. Jarman, 2000 Amos, a proneural gene for Drosophila olfactory sense organs that is regulated by lozenge. Neuron **25:** 69–78.

Heanue, T. A., R. Reshef, R. J. Davis, G. Mardon, G. Oliver *et al.*, 1999 Synergistic regulation of vertebrate muscle development by Dach2, Eya2, and Six1, homologs of genes required for Drosophila eye formation. Genes Dev. **13:** 3231–3243.

Heberlein, U., and K. Moses, 1995 Mechanisms of Drosophila retinal morphogenesis: the virtues of being progressive. Cell **81:** 987–990.

Heberlein, U., M. Mlodzik and G. M. Rubin, 1991 Cell-fate determination in the developing Drosophila eye: role of the rough gene. Development **112:** 703–712.

Heberlein, U., T. Wolff and G. M. Rubin, 1993 The TGF beta homolog dpp and the segment polarity gene hedgehog are required for propagation of a morphogenetic wave in the Drosophila retina. Cell **75:** 913–926.

Horsfield, J., A. Penton, J. Secombe, F. M. Hoffman and H. Richardson, 1998 Decapentaplegic is required for arrest in G1 phase during Drosophila eye development. Development **125:** 5069–5078.

Huang, M. L., C. H. Hsu and C. T. Chien, 2000 The proneural gene amos promotes multiple dendritic neuron formation in the Drosophila peripheral nervous system. Neuron **25:** 57–67.

Huang, Y., and J. A. Fischer-Vize, 1996 Undifferentiated cells in the developing Drosophila eye influence facet assembly and require the Fat facets ubiquitin-specific protease. Development **122:** 3207–3216.

Huang, Z., and S. Kunes, 1996 Hedgehog, transmitted along retinal axons, triggers neurogenesis in the developing visual centers of the Drosophila brain. Cell **86:** 411–422.

Jarman, A. P., Y. Grau, L. Y. Jan and Y. N. Jan, 1993 Atonal is a proneural gene that directs chordotonal organ formation in the Drosophila peripheral nervous system. Cell **73:** 1307–1321.

Jarman, A. P., E. H. Grell, L. Ackermann, L. Y. Jan and Y. N. Jan, 1994 Atonal is the proneural gene for Drosophila photoreceptors. Nature **369:** 398–400.

Jürgens, G., E. Wieschaus, C. Nüsslein-Volhard and H. Kluding, 1984 Mutations affecting the pattern of the larval cuticle in Drosophila melanogaster. Roux's Arch. Dev. Biol. **193:** 283–295.

Kawamura, K., T. Shibata, O. Saget, D. Peel and P. J. Bryant, 1999 A new family of growth factors produced by the fat body and active on Drosophila imaginal disc cells. Development **126:** 211–219.

Kopczynski, C. C., A. K. Alton, K. Fechtel, P. J. Kooh and M. A. Muskavitch, 1988 Delta, a Drosophila neurogenic gene, is transcriptionally complex and encodes a protein related to blood coagulation factors and epidermal growth factor of vertebrates. Genes Dev. **2:** 1723–1735.

Krämer, H., R. L. Cagan and S. L. Zipursky, 1991 Interaction of bride of sevenless membrane-bound ligand and the sevenless tyrosine-kinase receptor. Nature **352:** 207–212.

Kumar, J., and K. Moses, 1997 Transcription factors in eye development: a gorgeous mosaic? Genes Dev. **11:** 2023–2028.

Lee, E. C., X. Hu, S. Y. Yu and N. E. Baker, 1996 The scabrous gene encodes a secreted glycoprotein dimer and regulates proneural development in Drosophila eyes. Mol. Cell. Biol. **16:** 1179–1188.

Lee, J. J., D. P. von Kessler, S. Parks and P. A. Beachy, 1992 Secretion and localized transcription suggest a role in positional signaling for products of the segmentation gene hedgehog. Cell **71:** 33–50.

Lindsley, D. L., and G. G. Zimm, 1992 *The Genome of Drosophila melanogaster*. Academic Press, San Diego.

Ma, C., Y. Zhou, P. A. Beachy and K. Moses, 1993 The segment polarity gene hedgehog is required for progression of the morphogenetic furrow in the developing Drosophila eye. Cell **75:** 927–938.

Mardon, G., N. M. Solomon and G. M. Rubin, 1994 dachshund encodes a nuclear protein required for normal eye and leg development in Drosophila. Development **120:** 3473–3486.

Penton, A., S. B. Selleck and F. M. Hoffmann, 1997 Regulation of cell cycle synchronization by decapentaplegic during Drosophila eye development. Science **275:** 203–206.

Pignoni, F., B. Hu, K. H. Zavitz, J. Xiao, P. A. Garrity *et al.*, 1997 The eye-specification proteins So and Eya form a complex and regulate multiple steps in Drosophila eye development. Cell **91:** 881–891. (erratum: Cell **92**(4): following 585).

Powell, P. A., C. Wesley, S. Spencer and R. L. Cagan, 2001 Scabrous complexes with Notch to mediate boundary formation. Nature **409:** 626–630.

Ready, D. F., T. E. Hanson and S. Benzer, 1976 Development of the *Drosophila* retina, a neurocrystalline lattice. Dev. Biol. **53:** 217–240.

Renfranz, P. J., and S. Benzer, 1989 Monoclonal antibody probes discriminate early and late mutant defects in development of the Drosophila retina. Dev. Biol. **136:** 411–429.

Robertson, H. M., C. R. Preston, R. W. Phillis, D. M. Johnson-Schlitz, W. K. Benz *et al.*, 1988 A stable genomic source of P element transposase in *Drosophila melanogaster*. Genetics **118:** 461–470.

Robinow, S., and K. White, 1991 Characterization and spatial distribution of the ELAV protein during Drosophila melanogaster development. J. Neurobiol. **22:** 443–461.

Rubin, G. M., M. D. Yandell, J. R. Wortman, G. L. G. Miklos, C. R. Nelson *et al.*, 2000 Comparative genomics of the eukaryotes. Science **287:** 2204–2215.

Schupbach, T., and E. Wieschaus, 1991 Female sterile mutations on the second chromosome of *Drosophila melanogaster*. II. Mutations blocking oogenesis or altering egg morphology. Genetics **129:** 1119–1136.

Staehling-Hampton, K., P. D. Jackson, M. J. Clark, A. H. Brand and F. M. Hoffmann, 1994 Specificity of bone morphogenetic protein-related factors: cell fate and gene expression changes in *Drosophila* embryos induced by *decapentaplegic* but not *60A*. Cell Growth Differ. **5:** 585–593.

Strutt, D. I., and M. Mlodzik, 1997 Hedgehog is an indirect regulator of morphogenetic furrow progression in the Drosophila eye disc. Development **124:** 3233–3240.

Sun, Y., L. Y. Jan and Y. N. Jan, 1998 Transcriptional regulation of atonal during development of the Drosophila peripheral nervous system. Development **125:** 3731–3740.

Sun, Y., L. Y. Jan and Y. N. Jan, 2000 Ectopic scute induces Drosophila ommatidia development without R8 founder photoreceptors. Proc. Natl. Acad. Sci. USA **97:** 6815–6819.

Thomas, B. J., D. A. Gunning, J. Cho and S. L. Zipursky, 1994 Cell cycle progression in the developing Drosophila eye: *roughex* encodes a novel protein required for the establishment of G1. Cell **77:** 1003–1014.

Tomlinson, A., 1985 The cellular dynamics of pattern formation in the eye of Drosophila. J. Embryol. Exp. Morphol. **89:** 313–331.

Tomlinson, A., and D. F. Ready, 1987a Neuronal differentiation in the *Drosophila* ommatidium. Dev. Biol. **120:** 366–376.

Tomlinson, A., and D. F. Ready, 1987b Cell fate in the Drosophila ommatidium. Dev. Biol. **123:** 264–275.

Tomlinson, A., D. D. Bowtell, E. Hafen and G. M. Rubin, 1987 Localization of the sevenless protein, a putative receptor for positional information, in the eye imaginal disc of Drosophila. Cell **51:** 143–150.

Tomlinson, A., B. E. Kimmel and G. M. Rubin, 1988 rough, a Drosophila homeobox gene required in photoreceptors R2 and R5 for inductive interactions in the developing eye. Cell **55:** 771–784.

Tower, J., G. H. Karpen, N. Craig and A. C. Spradling, 1993 Preferential transposition of Drosophila P-elements to nearby chromosomal sites. Genetics **133:** 347–359.

Voelker, R. A., and C. H. Langley, 1978 Cytological localization of Roi (Rough eye). Dros. Inf. Serv. **53:** 185.

Wharton, K. A., K. M. Johansen, T. Xu and S. Artavanis-Tsakonas, 1985 Nucleotide sequence from the neurogenic locus notch implies a gene product that shares homology with proteins containing EGF-like repeats. Cell **43:** 567–581.

White, N. M., and A. P. Jarman, 2000 Drosophila atonal controls photoreceptor R8-specific properties and modulates both receptor tyrosine kinase and Hedgehog signalling. Development **127:** 1681–1689.

Wolff, T., and D. F. Ready, 1993 Pattern formation in the *Drosophila* retina, pp. 1277–1325 in *The Development of Drosophila Melanogaster*, edited by M. Bate and A. M. Arias. Cold Spring Harbor Laboratory Press, Cold Spring Harbor, NY.

Wright, T. R. F., R. B. Hodgetts and A. F. Sherald, 1976 The genetics of dopa decarboxylase in *Drosophila melanogaster*. Genetics **84:** 267–285.

Xu, T., and G. M. Rubin, 1993 Analysis of genetic mosaics in developing and adult Drosophila tissues. Development **117:** 1223–1237.

Zinn, K., L. McAllister and C. S. Goodman, 1988 Sequence analysis and neuronal expression of fasciclin I in grasshopper and Drosophila. Cell **53:** 577–587.

Communicating editor: T. Schüpbach